Optik 124 (2013) 6565–6569

Contents lists available at ScienceDirect

Optik

journal homepage: www.elsevier.de/ijleo

Two simple methods for overall determination of mobility in dynamic speckle patterns

N. Budini[a,b,*], C. Mulone[a], F.M. Vincitorio[a], C. Freyre[a], A.J. López[c], A. Ramil[c]

[a] Facultad Regional Paraná, Universidad Tecnológica Nacional, Avda. Almafuerte 1033, E3100XAI Paraná, Argentina
[b] Instituto de Desarrollo Tecnológico para la Industria Química, UNL-CONICET, Güemes 3450, S3000GLN Santa Fe, Argentina
[c] Universidade da Coruña, Centro de Investigacións Tecnolóxicas, Campus de Esteiro S/N, 15403 Ferrol, Spain

ARTICLE INFO

Article history:
Received 27 December 2012
Accepted 18 May 2013

Keywords:
Speckle
Dynamic speckle
Mobility
Biospeckle

ABSTRACT

In this work, we present two simple methods to quantify the mobility of dynamic speckle patterns. The first method is based on the averaged pixel intensity differences between subsequent frames, while the second simply counts the fraction of pixels whose intensity changes with time in more than a certain quantity related to background noise. We have analyzed the applicability of these methods to different specimens (inorganic and biological) and compared the results to check their validity.

1. Introduction

Speckle patterns formed by illuminating objects with a coherent light source are known to possess information about the object itself at a scale below that of the wavelength used (usually called interferometric precision) [1]. The variation or evolution of a pattern with time, i.e. a *dynamic* speckle pattern, allows further analysis of the object in the temporal domain [2]. A dynamic speckle pattern generally looks like "boiling" and its degree of activity is what we call, from now on, the speckle mobility (SM). If the object under study is of a biological kind, then the dynamic speckle pattern observed receives the name of *biospeckle*. In this case, the SM is termed biospeckle activity (BA) due to its relation to the biological activity of the specimen under investigation [3]. The quantification of BA is being increasingly investigated as a quality-control parameter for fruits and vegetables [4]. It has been generally observed that aging, bruising, infection or any other defect of fruits or vegetables are correlated with a diminished BA index [2]. However, a clear understanding, a consistent explanation and a standardized method to quantify this phenomenon are still lacking.

Commonly, in order to quantify and analyze the SM or the BA index of different specimens, the autocorrelation of the irradiance as a function of time is one of the employed methods [5,6]. However, there exists a wide variety of approaches such as the quantification of the speckle pattern's time history (THSP) by means of different descriptors like the inertia moment (IM) [3,7–10], the generalized differences (GD) method [11], the modified time correlation method [12], the time evolution inspection of the speckle pattern's texture [13–15], the contrast imaging method [16,17], the method of empirical mode decomposition [10,18], the Fujii difference method [19] and the analysis of the speckle pattern's phase evolution [20], among others. In the case of the Fujii and the GD methods, both of them provide a matrix of SM or BA values and not a single quantity or mobility index as is generally desired. Also, the resulting values of these methods are dependent upon eventual changes of the background illumination level, for which the Fujii method has a better performance. In turn, the IM method does provide a single value but is generally too sensitive to slight changes in the speckle pattern (even to noise) and, thus, any time-elapsed analysis becomes quite noisy. Besides this, the calculation of the IM index requires selecting a small portion (a row or a column) of the entire image which might not be representative of the object under study.

In this work we propose two different simple algorithms (which we call methods I and II from now on) for calculating the SM or BA index, aiming to overcome the mentioned disadvantages of the Fujii, the GD and the IM methods. Particularly, method I also allows reconstructing the image of the analyzed specimen in which different levels of SM or BA can be detected (similarly to Fujii or GD methods). We present the results obtained after applying these methods to some test cases in order to analyze the usefulness and trustiness of the developed algorithms.

* Corresponding author.
E-mail address: nbudini@intec.unl.edu.ar (N. Budini).

0030-4026/$ – see front matter © 2013 Elsevier GmbH. All rights reserved.
http://dx.doi.org/10.1016/j.ijleo.2013.05.119

2. Experimental

In order to test and validate the proposed algorithms we have used a standardized speckle recording experimental setup, which can be seen in Fig. 1. The sample under study is illuminated with a 30 mW He–Ne laser beam ($\lambda = 632.8$ nm), expanded by a 15 μm spatial filter. The resulting subjective speckle pattern is recorded by a 1-megapixel CMOS camera. In this way, the time evolution of the speckle pattern (biospeckle, in case of a biological specimen) can be digitally recorded. All images are digitally treated at an 8-bit grayscale resolution, i.e. the intensity of each pixel ranges from 0 (black) to 255 (white). The elapsed time analysis can be characterized by three parameters: (1) the number of frames, N (≥ 2), used to calculate the SM index at a given instant, (2) the period of time between those N frames, τ, whose lower limit is given by the highest temporal resolution attainable by the camera, generally much greater than the dynamic speckle correlation time ($<10^{-4}$ s, typically) [21], and (3) the period of time, t, between subsequent calculations of SM. Hence, each instant at which the calculation is performed has a finite temporal extension

$$\Delta\tau = (N-1)\tau \tag{1}$$

between the first and the last frame. This is also schematized in Fig. 1. Obviously, the condition $\Delta\tau < t$ must hold in order to make a valid analysis, i.e. without overlapped frames.

Image acquisition and analysis were performed by means of MATLAB® routines, specifically developed for this work.

3. Description of the methods

3.1. Method I

The first algorithm is based on both the generalized differences (GD) [11] and Fujii [19] methods. In GD, the SM is simply characterized by means of the following mathematical operation:

$$I(i,j) = \sum_{k=1}^{N-1} \left| I_{k+1}(i,j) - I_k(i,j) \right| \tag{2}$$

where $I(i, j)$ is the (i, j) component of the resulting BA matrix, N is the number of frames and $I_k(i, j)$ is the (i, j) component of the k-th image. The Fujii method, introduces a denominator of the form $|I_{k+1}(i,j) + I_k(i,j)|$ to the sum of Eq. (2) in order to compensate for fluctuations of the illumination level during image acquisition. Our first method consists on averaging the differences of Eq. (2). Mathematically this is expressed as

$$I(i,j) = \sum_{k=1}^{N-1} \frac{\left| I_{k+1}(i,j) - I_k(i,j) \right|}{N-1} \tag{3}$$

and is equivalent to inspecting how different, on average, is each image as compared to the next one in the time sequence. This gives as a result a new image, I, which serves both as a SM map and as a reconstruction of the specimen image in a similar way of Fujii and GD methods. To get a single SM index and quantify the general degree of mobility of the dynamic speckle pattern, the values corresponding to each pixel of the image emerging from Eq. (3) are also averaged. This can be expressed as

$$\begin{aligned} SM_I &= \frac{1}{mn} \sum_{i}^{m} \sum_{j}^{n} I(i,j) \\ &= \frac{1}{mn} \sum_{k=1}^{N-1} \frac{1}{N-1} \sum_{i}^{m} \sum_{j}^{n} \left| I_{k+1}(i,j) - I_k(i,j) \right| \end{aligned} \tag{4}$$

where SM_I stands for the SM index resulting from method I and m and n are the number of rows and columns of I, respectively. Hence, the SM_I index measures the image-to-image area averaged pixel intensity changes. This procedure resembles the temporal difference method proposed by Martí-López et al. [22] but differs from it in the averaging step over the whole set of N images from which the SM_I index is extracted, as stated in Eq. (3).

3.2. Method II

Our second method simply measures the average fraction of pixels whose intensity changes as a function of time from image to image in more than a certain amount, which we call *speckle noise*. If a speckle pattern is ideally static, i.e. if there is no mobility at all, this fraction would be obviously zero. In the real case, each speckle pattern, whether static or dynamic, is affected by some degree of noise coming from different sources (vibrations, ambient dust, electronics, thermal fluctuations, and so on). It is possible to inspect the amount of noise of the acquisition system by measuring the variation of pixel intensity in a speckle pattern which is known that should be static. In this way, we estimate the noise level, r, by means of taking the maximum absolute intensity variation between the N images used to calculate the SM index. Mathematically this can be expressed as

$$r = \max\left(\left| I_{k+1}^{static}(i,j) - I_k^{static}(i,j) \right| \right) \tag{5}$$

where k covers all possible values from 1 to $N-1$ and i and j cover all m rows and n columns of each image, respectively. The "static" superscript makes reference to the fact that this calculation has to be performed on a sequence of N images of a speckle pattern that is supposed to be static. In practice, it suffices to make the calculation of Eq. (5) in a region of the images under analysis that should not change with time. Once the noise level is known, the algorithm proceeds by (i) calculating the $N-1$ differences $|I_{k+1}(i,j) - I_k(i,j)|$ as in method I, (ii) counting the amount of pixels whose intensity varies in more than the threshold value r and (iii) averaging this quantity. This operation can be expressed concisely as

$$SM_{II} = \frac{1}{mn} \sum_{k=1}^{N-1} \frac{1}{N-1} \sum_{i=1}^{m} \sum_{j=1}^{n} \Theta\left[\left| I_{k+1}(i,j) - I_k(i,j) \right| - r \right] \tag{6}$$

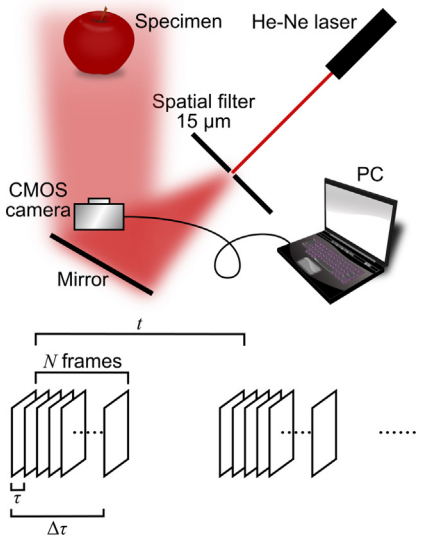

Fig. 1. Standard experimental setup used to acquire the speckle image sequence. A spatially filtered He–Ne laser beam illuminates the sample under analysis and a CMOS camera captures the generated speckle patterns.

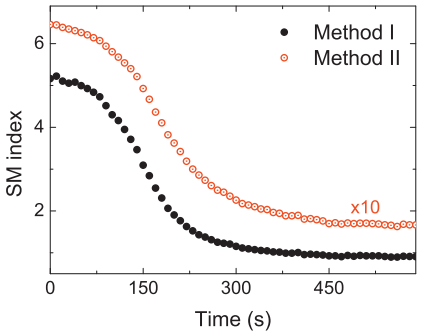

Fig. 2. Time evolution of the net SM_I and SM_{II} values for the nail polish. SM_{II} values were rescaled ($\times 10$), so both curves fit in the same graph. The data points clearly follow a decreasing sigmoidal curve, reaching a constant value when the nail polish dries.

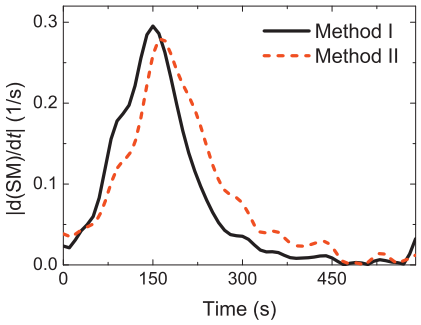

Fig. 4. Absolute value of the SM index's rate of change, $|\mathrm{d}(SM)/\mathrm{d}t|$, obtained from the curves presented in Fig. 2. Both methods have a maximum rate of change at almost the same time and decrease to zero simultaneously for times above 300 s, when the nail polish dries.

where SM_{II} stands for the SM index resulting from method II, the scaling factor $(mn)^{-1}$ transforms the obtained quantity to the desired area fraction of varying pixels and $\Theta(x)$ is the well-known Heaviside function, defined as

$$\Theta(x) = \begin{cases} 1 & \text{if } x > 0 \\ 0 & \text{if } x < 0 \end{cases} \tag{7}$$

4. Results and discussion

In order to analyze the performance of both methods, we have selected different test cases. Firstly, we sought for a specimen underlying some transformation in which we could anticipate that the SM index should decay with time. A phenomenon where this condition is clearly satisfied is, for example, the drying of paint. Hence, we have analyzed the drying of a generic nail polish. As a first experience we fixed the image acquisition parameters to $N = 10$ frames, $t = 10$ s and $\tau = 1$ s, where this latter value is the greatest possible in order to satisfy the condition $\Delta\tau < t$. The corresponding evolution with time of the resulting net SM_I and SM_{II} values is presented in Fig. 2. The values corresponding to method II were rescaled ($\times 10$), so the evolution for both methods fits in the same graph (we recall here that the SM_{II} index lies in the range between 0 and 1). The data points clearly follow a decreasing sigmoidal curve, reaching constant values when the polish dries. These values correspond to the speckle background mobility level as detected by each method, and in some way give an idea of each method's sensitivity.

Fig. 3 shows the corresponding normalized curves of Fig. 2. Normalization to the respective maximum values was performed in order to further compare both methods.

By inspecting these curves, one is tempted to estimate how much time would take the nail polish to dry. At a first glance, it seems appropriate to extrapolate the almost linear part of the decaying curve until intersecting the time axis. By doing this, we got periods of approximately (282 ± 10) and (370 ± 15) s for methods I and II, respectively. A moderate to high discrepancy of 30% is observed between both values, averaging to about (320 ± 12) s. Besides this, by analyzing the absolute value of the SM index's rate of change, i.e. $|\mathrm{d}(SM)/\mathrm{d}t|$, we observed that both methods present similar behaviors as shown in Fig. 4.

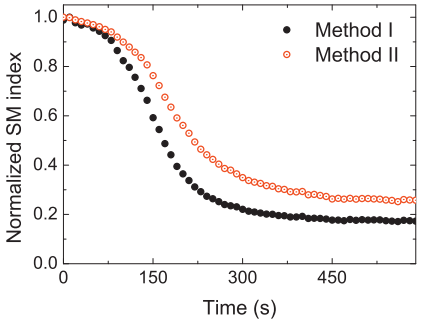

Fig. 3. Further comparison between the curves of Fig. 2, which were normalized to their corresponding maximum values.

The curves are quite similar and present a maximum at almost the same time, differing by only 15 s. Also, the rate of change of both methods approaches to zero for times slightly above 300 s, where the drying process of the nail polish can be considered as completed. This value is quite similar to the average of the estimated drying times derived from methods I and II by means of extrapolating the linear portion of the curves. Therefore, despite the difference between the SM values obtained, the rate of change can be considered as being the same in both cases.

We have also checked the proper functioning of the algorithms and the validity of the results by comparing the obtained evolution curves with those obtained by, for example, the IM method. This method consists in selecting a single row or column of the dynamic speckle images to conform the time history speckle pattern (THSP) for that region. Subsequently, a 256×256 elements co-occurrence matrix (CO) is calculated in which the (i, j) component value equals the amount of times that the j gray value follows the i gray value in the THSP. Finally, the speckle activity value is calculated as the moment of inertia of the co-occurrence matrix as

$$IM = \sum_{i,j} CO(i,j)(i-j)^2 \tag{8}$$

In Fig. 5 we present an example of the evolution curve obtained for the SM index by this procedure, from the constructed THSP figures of a test sample with a clear decreasing mobility as a function of time.

In turn, in Fig. 6 we present the time evolution of the IM values for the drying nail polish under study. The calculated values result quite noisy, but the data points oscillate around a typical sigmoidal curve which was fitted by a least-squares procedure and is presented as a guide to the eye. The inset compares this curve, after being normalized, to those fitted analogously to the normalized data points obtained by methods I and II. All curves present the same decreasing trend, which indicates that the proposed algorithms represent quite adequately the overall mobility in the dynamic speckle pattern of the specimen under study.

As other test cases we have selected two biological specimens: an apple and a strawberry. Now, for biological specimens, we use the names BA_I and BA_{II} instead of SM_I and SM_{II}, respectively. Both fruits were left at room temperature during observations. In the case of the apple, we proceeded to cut it in a half and focus the camera to a region of its pulp. The acquisition parameters where

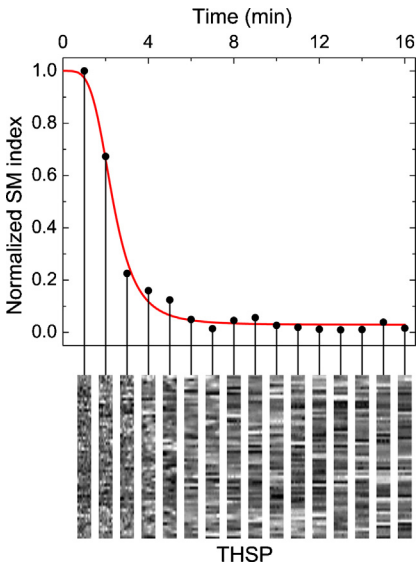

Fig. 5. Example of the evolution curve for the SM index of a test sample calculated by the IM method. The sequence of images shown below corresponds to the THSP matrices for each point, from which the SM index is obtained.

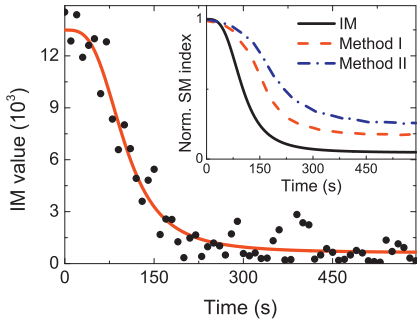

Fig. 6. Time evolution of the SM values obtained by the IM method for the drying nail polish. The data points result quite noisy, but oscillate around a sigmoidal curve. The curve was fitted by a least-squares procedure and is presented to guide the reader's eye.

$N = 10$ frames, $t = 300$ s and $\tau = 1$ s, therefore the condition $\Delta\tau < t$ is more than satisfied. Fig. 7 presents the normalized curves of the time evolution of BA_I and BA_{II} indexes of the apple, obtained by both methods. The exponentially decaying trend is attributed to a mixture of the oxidizing and drying processes that the pulp undergoes when exposed to air. Both methods show the same behavior of the apple's pulp.

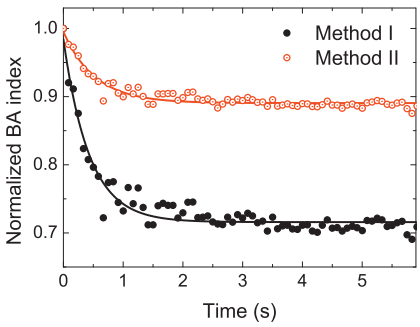

Fig. 7. Normalized curves of the BA_I and BA_{II} indexes obtained for the apple's pulp. An exponentially decaying trend is observed on both curves, which is attributed to a mixture of the oxidizing and drying processes undergoing on the pulp when exposed to air.

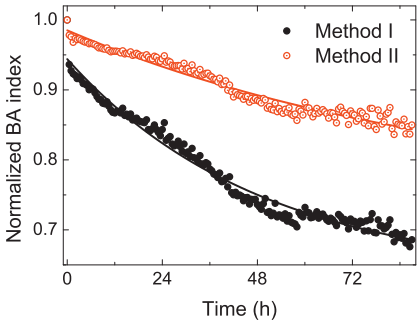

Fig. 8. Time evolution of the curves obtained by methods I and II in the case of the strawberry. The data points also follow an approximate exponential decay. It is worth noting that the points oscillate around the fitted curve. This behavior is attributed to periodic oscillations of humidity during the observation, since it covers both day and night hours.

The strawberry was analyzed with the acquisition parameters $N = 10$ frames, $t = 30$ min and $\tau = 1$ s during a period of 87 h (≈3.5 days). The time evolution of the curves obtained by both methods is presented in Fig. 8. Despite the fact that the data points also follow an approximate exponential decay, it is worth noting the presence of some kind of oscillation around a mean curve. We attribute this behavior to periodic oscillations of room temperature and/or humidity during the observation's lapse time, since it covers both day and night hours.

As can be evidenced from the above results, the proposed methods correctly represent the mobility variations of the dynamic speckle patterns for different specimens (biological or not). For the nail polish case we obviously expected the SM index to decay with time, and this assumption was in accordance with the results. For the biological specimens, we also expected a decaying BA index but with some degree of random behavior due to the stochastic nature of biological processes. Thus, we could also confirm this latter assumption by means of the proposed methods. The complex phenomena involved in biological specimens, translated in speckle pattern mobility under coherent illumination, are not easily describable in terms of their relation with physical parameters. However, we have found a clear correlation between the BA indexes, calculated by methods I and II, and humidity. A detailed analysis of this and other possible correlations exceeds the aim of this work and will be addressed in future works.

5. Conclusion

We have presented two simple methods for calculating the overall speckle pattern mobility of a sequence of images acquired by a standard CMOS camera. After a detailed description of the ideas behind each method and of the required calculation steps, we proceeded to analyze some selected test cases. At first, we analyzed the evolution of SM in an inorganic sample with a predictable outcome, i.e. the drying of a commercial nail polish. This test case served us to inspect several aspects of the algorithms in order to improve them from their origin, until reaching the final form presented in this work. However, further improvements might be introduced after application of the methods to different specimens. As presented, the methods proved to correctly describe the expected trends of speckle pattern's mobility for the selected test cases. Besides this, after comparing the curves of the nail polish with that obtained by the well-known IM method we could check the validity of the results. Concerning the biological specimens, an apple and a strawberry, we also observed a decaying trend of the BA values, but with some degree of randomness attributed to the stochastic nature of biological processes. This is in accordance with previous knowledge about BA of fruits. In the case of the strawberry, analyzed during

more than three days, we have detected a clear correlation between BA and humidity. However, this latter point will be addressed in future research. The proposed methods are based on simple and logic assumptions, are simple to implement and describe correctly the evolution of the overall speckle pattern mobility of selected test cases.

Acknowledgments

This work was funded by joint projects from Universidad Tecnológica Nacional and CONICET, of Argentina, and Universidade da Coruña, of Spain.

References

[1] R. Jones, C. Wykes, Holographic and Speckle Interferometry, Cambridge University Press, Cambridge UK, 1989.
[2] H.J. Rabal, R.A. Braga Jr., Dynamic Laser Speckle and Applications, CRC Press, Taylor & Francis Group, Boca Ratón, FL, USA, 2009.
[3] R.A. Braga Jr., B.O. Silva, G. Rabelo, R.M. Costa, A.M. Enesa, N. Cap, H.J. Rabal, R. Arizaga, M. Trivi, G. Horgand, Opt. Laser Eng. 45 (2007) 390.
[4] A. Kurenda, A. Adamiak, A. Zdunek, Postharvest Biol. Technol. 67 (2012) 118.
[5] Y. Aizu, T. Asakura, Opt. Laser Technol. 23 (1991) 205.
[6] B. Ruth, J. Mod. Opt. 34 (1987) 257.
[7] A. Oulamara, G. Tribillon, J. Duvernoy, J. Mod. Opt. 36 (2000) 165.
[8] R. Arizaga, M. Trivi, H.J. Rabal, Opt. Laser Technol. 31 (1999) 163.
[9] R.A. Braga, W.S. Silva, T. Sáfadi, C.M.B. Nobre, Opt. Commun. 281 (2008) 2443.
[10] A. Federico, G.H. Kaufmann, Opt. Commun. 267 (2006) 287.
[11] R. Arizaga, N. Cap, H.J. Rabal, M. Trivi, Opt. Eng. 41 (2002) 287.
[12] J.A. Pomarico, H.O. DiRocco, Rev. Sci. Instrum. 75 (2004) 4727.
[13] M. Fernández, A. Mavilio-Núñez, H.J. Rabal, M. Trivi, App. Opt. 41 (2002) 6745.
[14] A. Mavilio-Núñez, M. Fernández, M. Taño, H.J. Rabal, R. Arizaga, M. Trivi, Opt. Eng. 46 (2007) 057005.
[15] A. Mavilio-Núñez, M. Fernández, M. Trivi, H.J. Rabal, R. Arizaga, Signal Process. 90 (2010) 1623.
[16] J.D. Briers, Opt. Quant. Electron. 10 (1978) 364.
[17] J.D. Briers, S. Webster, J. Biomed. Opt. 2 (1996) 174.
[18] S. Equis, P. Jacquot, Strain 46 (2008) 550.
[19] H. Fujii, K. Nohira, Y. Yamamoto, H. Ikawa, T. Ohura, App. Opt. 26 (1987) 5321.
[20] H.J. Rabal, N. Cap, M. Trivi, R. Arizaga, A. Federico, G.E. Galizzi, G.H. Kaufmann, App. Opt. 45 (2006) 8733.
[21] P. Zakharov, A.C. Völker, M.T. Wyss, F. Haiss, N. Calcinaghi, C. Zunzunegui, A. Buck, F. Scheffold, B. Weber, Opt. Expr. 17 (2009) 13904.
[22] L. Martí-López, H. Cabrera, R.A. Martínez-Celorio, R. González-Peña, Opt. Commun. 283 (2010) 4972.